

See discussions, stats, and author profiles for this publication at: <https://www.researchgate.net/publication/260251413>

Etch free graphene transfer to polymers

ARTICLE in SURFACE AND COATINGS TECHNOLOGY · FEBRUARY 2014

Impact Factor: 2 · DOI: 10.1016/j.surfcoat.2013.10.080

CITATIONS

3

READS

128

12 AUTHORS, INCLUDING:



[Scott W. Schmucker](#)

Zyvex Labs

22 PUBLICATIONS 274 CITATIONS

SEE PROFILE



[Joshua David Caldwell](#)

United States Naval Research Laboratory

147 PUBLICATIONS 1,072 CITATIONS

SEE PROFILE



[Jeremy T Robinson](#)

United States Naval Research Laboratory

96 PUBLICATIONS 2,552 CITATIONS

SEE PROFILE



[Boris Feigelson](#)

United States Naval Research Laboratory

74 PUBLICATIONS 458 CITATIONS

SEE PROFILE

High-Quality Uniform Dry Transfer of Graphene to Polymers

Evgeniya H. Lock,^{*,†} Mira Baraket,[†] Matthew Laskoski,[‡] Shawn P. Mulvaney,[‡] Woo K. Lee,[‡] Paul E. Sheehan,[‡] Daniel R. Hines,[§] Jeremy T. Robinson,^{||} Jacob Tosado,[⊥] Michael S. Fuhrer,[⊥] Sandra C. Hernández,[†] and Scott G. Walton[†]

[†]Plasma Physics Division and [‡]Chemistry Division, Naval Research Laboratory, Washington, DC 20375, United States

[§]Laboratory for Physical Sciences, University of Maryland, College Park, Maryland 20740, United States

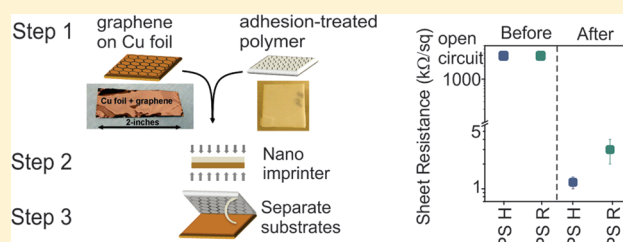
^{||}Electronics Division, Naval Research Laboratory, Washington, DC 20375, United States

[⊥]Center for Nanophysics and Advanced Materials, University of Maryland, College Park, Maryland 20742, United States

S Supporting Information

ABSTRACT: In this paper we demonstrate high-quality, uniform dry transfer of graphene grown by chemical vapor deposition on copper foil to polystyrene. The dry transfer exploits an azide linker molecule to establish a covalent bond to graphene and to generate greater graphene–polymer adhesion compared to that of the graphene–metal foil. Thus, this transfer approach provides a novel alternative route for graphene transfer, which allows for the metal foils to be reused.

KEYWORDS: Graphene, transfer print, polystyrene, Raman spectroscopy



Interest in organic electronics stems from the low inherent cost of plastics, and the relative ease of processing organic compounds.¹ Organic electronic materials have been successfully applied in organic light-emitting devices (OLEDs),² thin-film transistors (TFTs),^{3,4} and thin film organic photovoltaic cells.⁵ Flexible electronic devices typically rely on the conducting properties of small molecules, conductive polymers, or biological materials. However, their inherent low carrier mobilities ($<1 \text{ cm}^2 \text{ V}^{-1} \text{ s}^{-1}$),⁶ low electrical conductivity ($\sigma \sim 10^{-6} \text{ S cm}^{-1}$), and low charge carrier velocity (10 cm s^{-1})⁷ represent serious limitations and underline the need for a transparent conductor that will retain the flexibility of organics while achieving higher carrier mobilities. Graphene has emerged as this long-sought conductor due to its zero-band gap, extremely high electron mobilities of $10\,000\text{--}70\,000 \text{ cm}^2 \text{ V}^{-1} \text{ s}^{-1}$,⁸ and low absorption (2.3%) in the visible spectrum.⁹ The merger of graphene and plastics holds promise for the production of flexible touch screens, displays, and smart windows.^{9–12} However, a truly manufacturable process in any of the aforementioned applications requires controlled, uniform graphene growth and precise graphene placement on top of organic surfaces, along with the development of cost-effective techniques for organic device fabrication.

Large-area graphene is typically produced via thermal graphitization of SiC, or chemical vapor deposition (CVD) on metals substrates^{13,14} with the latter promising lower cost and greater scalability to large areas. To fabricate devices, graphene must then be transferred to a semiconductor or plastic substrate. The current graphene transfer procedures rely on polymer coating^{15–17} or thermal release tape^{14,18–20} to maintain the graphene film integrity and to prevent folding

while the underlying Cu foil is chemically etched. In this paper, we demonstrate an alternative strategy to transfer graphene directly to a polymeric substrate. A flowchart describing the graphene transfer print method is shown in Figure 1. In the first step, graphene was grown via CVD on a copper foil, and separately the polymer surface was treated to enhance its adhesion to graphene. The latter process involved plasma-based surface activation and the deposition of *N*-ethylamino-4-azidotetrafluorobenzoate (TFPA-NH₂) linker molecule. In the second step, the TFPA treated polymer surface was placed in contact with graphene-covered copper foil and printed, under heat and pressure, in a NX 2000 Nano Imprinter. In the final step, the polymer substrate with attached graphene was separated from the metal foil. Each of these steps will be discussed in greater detail below.

First, graphene was grown on a Cu foil using previously reported parameters.¹³ The film was then transferred to a $1 \text{ cm} \times 1.5 \text{ cm}$ polystyrene substrate, which was treated to enhance its adhesion properties. Polystyrene (PS) was chosen because it is a well-characterized polymer with simple chemical composition and therefore can serve as a model substrate to understand the requirements for graphene transfer.

Polystyrene was also an appropriate choice because in its native state its adhesion to graphene is low. Thus, the surface chemistry of the polystyrene may be systematically varied to enhance adhesion to graphene and ensure transfer. The first step in controlling the adhesion was polymer functionalization

Received: September 2, 2011

Revised: November 23, 2011

Published: November 30, 2011

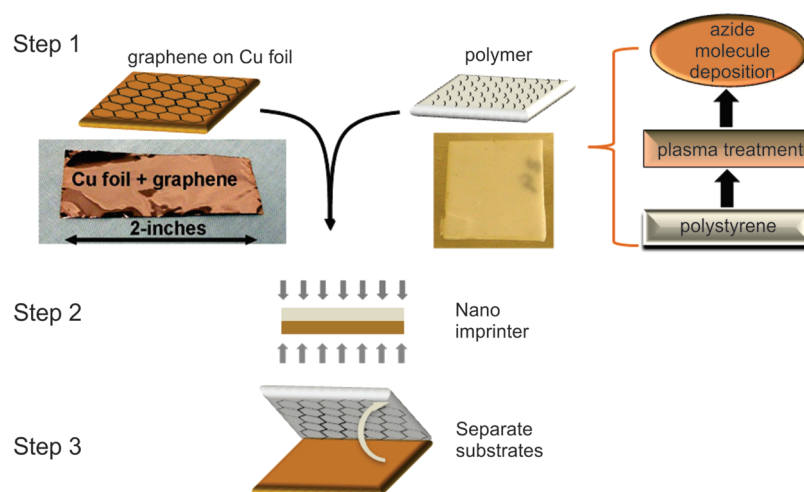


Figure 1. Flowchart of the transfer process. In step 1, graphene film was grown on Cu foil, and independently the polymer surface was treated to increase reactivity. In step 2, both substrates were placed in a NX 2000 Nano Imprinter. In step 3, the substrates were separated and graphene was transferred to the polymer.

by low energy electron beam-generated plasma. These plasmas have been shown to functionalize only the terminal surface of the polymer without etching.²¹ A one minute exposure to carbon dioxide plasma was sufficient to introduce oxygen functional groups including hydroxyls, carboxyls, and carbonyls (see Supporting Information). However, plasma functionalization alone was found to be insufficient for transfer. So, to enhance adhesion after plasma treatment an azide linker molecule was deposited on the polymer for two hours by dip coating since azides provide strong covalent bonds to graphene.²² The terminal azide functionality enabled the *N*-ethylamino-4-azidotetrafluorobenzoate (TFPA-NH₂) linker molecule to bind directly with graphene through a carbene bond. It should be noted that polymer substrates require more care than typical inorganic materials. Specifically, polymers will dissolve in organic solvents including acetone, hexane, toluene, and so forth and so the solvent for reacting the azide molecule has to be mild enough to not degrade the polymer during dip coating. In this work, TFPA-NH₂ was chosen since it is soluble in methanol and allows for a large range of organics to be used as substrates for graphene transfer.

To design TFPA/polymer interface with high adhesive strength two different attachment protocols were developed. In the first approach, the TFPA molecule was attached to the plasma-functionalized polymer surfaces via its amine end group to carboxyl and hydroxyl groups on the basis of hydrogen bond (acid–base interactions) (Figure 2a, hereafter referred to as PS H). In the second, the carboxyl groups present on the polymer surface were reacted with EDC/NHS to form a covalent amide bond between the TFPA and the polymer (Figure 2b, hereafter referred to as PS R). As a control, unmodified PS substrate was also printed against graphene on Cu foil (hereafter referred to as PS ref).

In the second step of the transfer method (Figure 1), the TFPA-treated polymer surface was placed in contact with graphene-covered Cu foil and printed in a NX 2000 Nano Imprinter at a pressure of 500 psi for 30 min. The azide terminal group of TFPA-NH₂ molecule, which was inactive during linker molecule deposition, was heat activated and a covalent carbene bond between graphene and TFPA was formed. In the third and final step of the transfer method, the polymer substrate with attached graphene was separated from

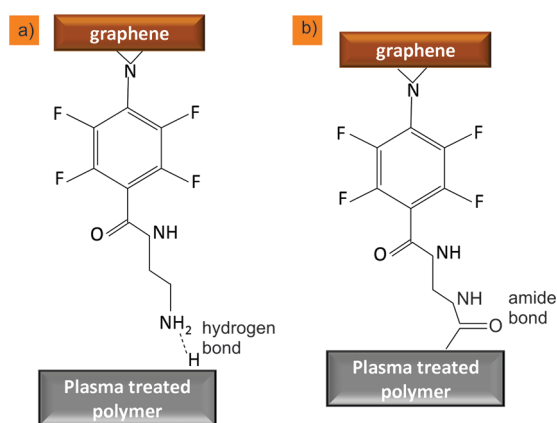


Figure 2. Attachment schematic. (a) (PS H) hydrogen bond attachment between the amine groups of the TFPA and the hydroxyls and carboxyl groups of the plasma treated polystyrene surface; (b) (PS R) covalent bond attachment between TFPA and the plasma treated polystyrene surface. To form an amide bond the carboxyl groups on the polymer surface were reacted with NHS-EDC chemistry prior to TFPA deposition.

the metal foil. The total graphene transfer time including plasma treatment, dip coating, and printing was less than three hours, although it may be reduced. For example, by using UV light the azide group activation time can be reduced to five minutes.²³ Further optimization in the other steps might be possible as well. It should be noted that all steps in this method (graphene synthesis on Cu foil, plasma treatment of plastics, and the following dip coating step) are scalable, and so there is no limitation to the size of graphene films that can be transferred.

Raman spectroscopy and microRaman mapping confirmed the transfer of graphene to polystyrene and measured the uniformity of the graphene film. As shown in Figure 3, graphene was transferred to PS H and PS R as signified by the appearance of the 2D peak on the TFPA-treated polystyrene and the absence of that peak on the Cu foil after print. A comparison of PS H with graphene transferred onto SiO₂/Si substrates using the conventional wet chemical approach (Figure 3c) indicates that the 2D graphene peak on PS

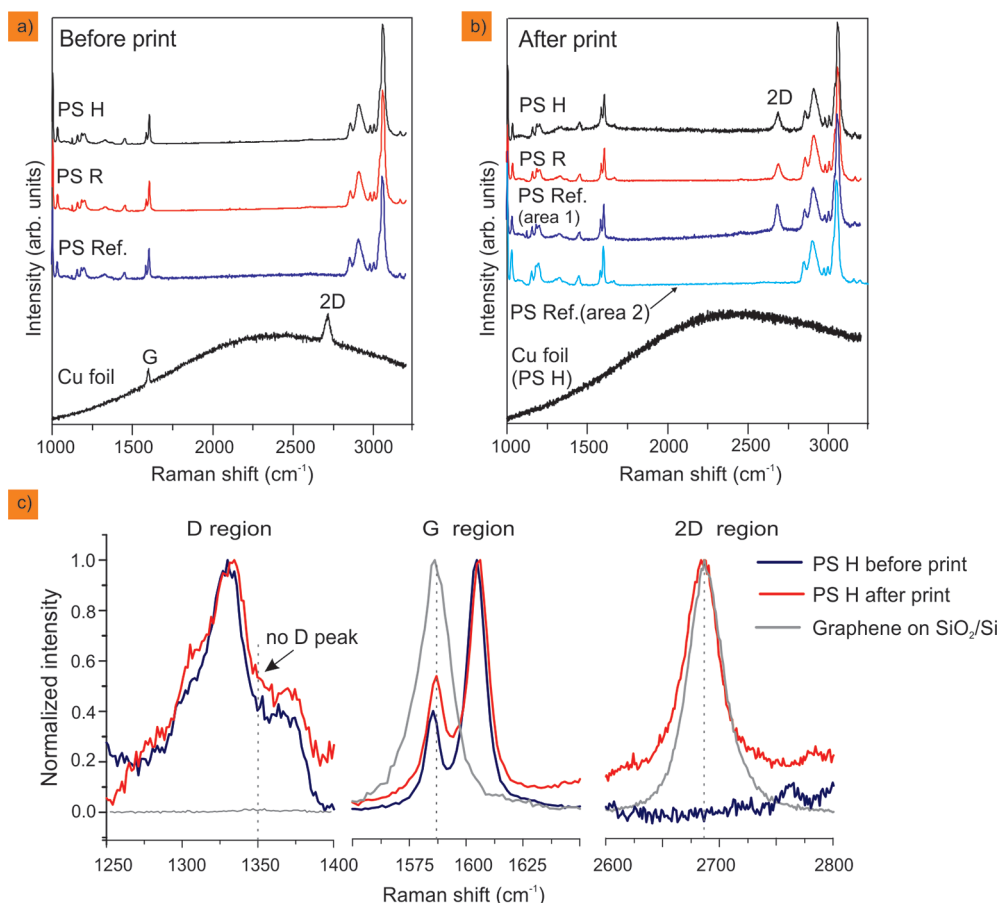


Figure 3. Raman spectra of polystyrene surfaces. Panels (a) and (b) show PS ref, PS H, PS R, and Cu foil before and after print, respectively. Panel (c) shows high-resolution D, G, and 2D regions of PS H before and after print. As a reference, graphene on SiO_2/Si substrate is included.

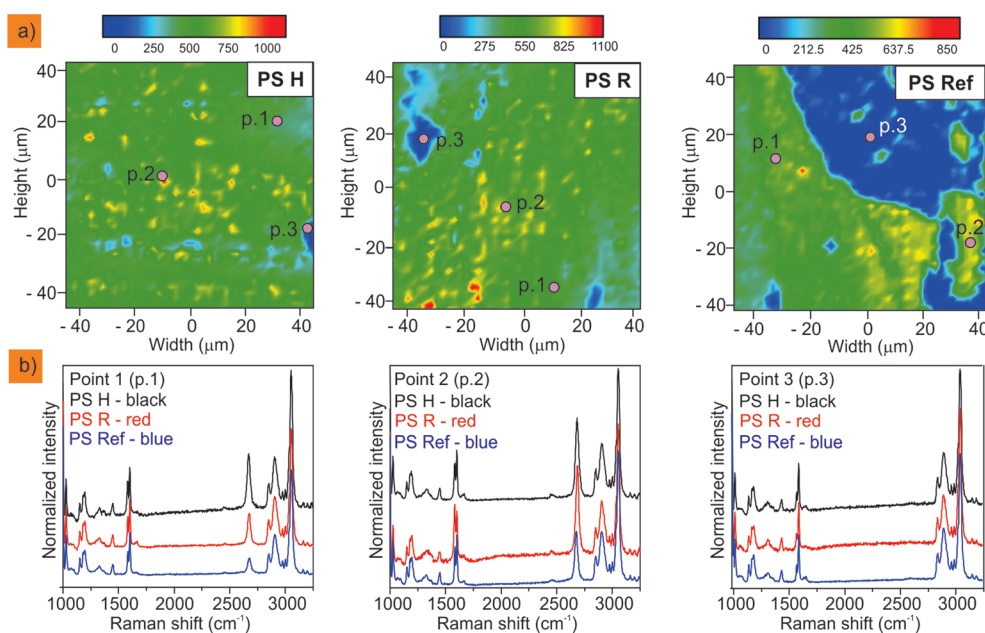


Figure 4. Microraman maps (a) of PS H, PS R, and PS ref after print and the corresponding Raman spectra at chosen points (b) of each map.

matches the peak position (2686 cm^{-1}) and peak width (23 cm^{-1}) of graphene/ SiO_2/Si . Thus, the graphene printed onto the polymer substrate is of high quality and single layer.^{24,25} In the regions of the D- and G-peak of graphene, polystyrene shows several Raman modes that obscure the observation of the

graphene modes. However, an increase of peak height at the 1586 cm^{-1} is clearly visible and indicative of the graphene G-peak. A closer look at the D region revealed no change of the shape of the peak around 1350 cm^{-1} , suggesting negligible D peak and thus no significant increase in point defects in the

graphene layer during transfer. This is perhaps surprising because the covalent bonding of the linker molecule to graphene may be expected to act as a point defect. Interestingly, the signature graphene peaks were detected on some areas of the unmodified sample as well (Figure 3b, PS ref area 1). This might be because the printing temperature is above the glass transition temperature allowing for good conformal contact at the polymer/graphene interface.

The micro-Raman maps (Figure 4a) of the 2D peak over about $800\ \mu\text{m}^2$ area show uniform coverage for PS H and PS R. This was not true for PS ref where large areas with no graphene were detected. It should be noted that the polymer surface roughness (rms) after print was $\sim 1\ \mu\text{m}$, comparable to the depth of field of the Raman microprobe. Thus, intensity variation over large areas is not surprising. To better characterize this phenomenon, we analyzed individual Raman spectra of many selected points (examples are shown in Figure 4b) and concluded that intensity lower than 200 (dark blue color in Figure 4a) corresponds to bare polymer and intensity above 200 corresponds to transferred graphene while the variations in intensity (light blue to red color in Figure 4a) reflects the variation in height. Alternatively, the uniformity of the transferred graphene layer on macroscale can be evaluated by analyzing the graphene residuals on the Cu foil after transfer printing (see Supporting Information). This was accomplished by transferring the residuals from the printed Cu foil to Si using the wet transfer process. It is clear from both methods that full transfer of graphene onto the PS H and PS R substrates was achieved, while for the reference sample (PS ref) only a partial transfer was observed.

Samples were electrically characterized using a standard 4-point probe station with 1 mm spaced probe tips. Figure 5

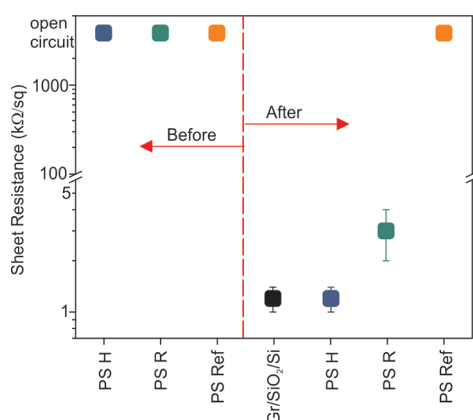


Figure 5. Sheet resistance before and after print of polystyrene samples.

shows the 4-probe sheet resistance of the samples before and after graphene transfer. The insulating polymer surface was indeed found to be conducting after transfer with low sheet resistances of 1 (PS H) and 3 $\text{k}\Omega/\text{sq}$ (PS R). These values are consistent with the sheet resistance ($\sim 1\ \text{k}\Omega/\text{sq}$) of monolayer graphene transferred to PET and SiO_2/Si .^{15,17,26} The reference sample (PS ref) did not show measurable conductivity, which is consistent with incomplete graphene transfer.

The electrical conductivity, carrier densities and mobilities of the transferred graphene films for PS H and PS R were determined by Hall measurements using copper pressure clips in a van der Pauw configuration over areas of $0.5 \times 0.5\ \text{mm}^2$.

The measured conductivities were increased from $\sim 10^{-6}\ \text{S/m}$ before print to $\sim 5 \times 10^5\ \text{S/m}$ after print. The carrier densities for PS R and PS H were 1.6×10^{13} and $5.6 \times 10^{12}\ \text{cm}^{-2}$, respectively, with corresponding mobilities of $1140 \pm 71\ \text{cm}^2/(\text{V s})$. These values are consistent with previously reported values for graphene transferred from SiC to SiO_2/Si ¹⁸ and the calculated values for graphene transferred from Cu foils to glass,²⁶ suggesting the developed transfer method provides a promising route for graphene transfer to organics.

In summary, we have demonstrated a unique dry approach for graphene transfer from copper foil to polystyrene based on enhanced adhesion using azide-based linker molecule. The Cu foil was not chemically etched and thus it can be reused for sequential graphene growth. The graphene monolayer transferred to the treated polymer was uniform and of high quality as signified by a narrow 2D peak width ($23\ \text{cm}^{-1}$), low sheet resistance (1–3 $\text{k}\Omega/\text{sq}$), high carrier densities ($> 5 \times 10^{12}\ \text{cm}^{-2}$), and good mobilities ($1140\ \text{cm}^2/(\text{V s})$). The size of the transferred area is limited only by the size of the growth Cu foil and the polystyrene sheet. In principle, this method can be applied to transfer graphene to a wide range organic or inorganic substrates. Similarly, transfer from other growth substrates could be possible as well.

Methods. Materials. Polystyrene films with a thickness of $250\ \mu\text{m}$ were purchased from Tekra. The 1-ethyl-3-[3-dimethylaminopropyl]carbodiimide hydrochloride (EDC) and N-hydroxysuccinimide (NHS) were purchased from Thermo Fisher Scientific. The 2-[morpholino]ethanesulfonic acid (MES), NaCl, and sodium phosphate were purchased from Sigma Aldrich. The activation buffer was composed of 0.1 M MES, 500 mM NaCl, and the pH was adjusted to 6.0. The coupling buffer was made from 100 mM sodium phosphate, 150 mM NaCl, and the pH was adjusted to 7.2.

Plasma Treatment. Electron beam-generated plasma was used for polymer functionalization. The electron beam was produced by applying a $-2\ \text{kV}$ pulse to a linear hollow cathode for a selected pulse width and duty factor. The emergent beam passed through a slot in a grounded anode and was then terminated at a second grounded anode located further downstream. The electron beam volume between the two anodes defines the ionization source volume with the dimensions set by the slot size ($1 \times 25\ \text{cm}^2$) and the anode-to-anode length (40 cm). Beam spreading from collisions with the background gas was suppressed by a coaxial magnetic field (150 G) produced by a set of external coils. Because the beam is collimated, few high energy electrons strike the surface of the material. The system vacuum was maintained by a 250 L/s turbo pump with a base pressure of 5×10^{-6} Torr. The operating pressure was achieved by introducing CO_2 (purity $> 99.995\%$) through the mass flow controllers and throttling the pumping speed using a manual gate valve. The samples were placed on a 10.2 cm diameter stage located at 2.5 cm from the nominal edge of the electron beam. The stage was held at ground potential and room temperature. Polymers were treated at a pressure of 100 mTorr, for 1 min, at a duty factor of 10%. To take advantage of the increased chemical reactivity of the polystyrene surface, plasma treated samples were used within 24 h after treatment.

Amine Tetrafluoroazide Synthesis. All starting materials were of reagent grade and used without further purification. N-succinimidyl-4-azidotetrafluorobenzoate was synthesized from a previously published procedure [ref]. ^1H NMR was performed on a Bruker ADVANCE 300 spectrometer. N-ethylamino-4-

azidotetrafluorobenzoate (**1**): To a 250 mL round-bottom was added ethylenediamine (6.36 g, 105.8 mmol) and 100 mL acetonitrile. The mixture was cooled to 0 °C and (N-succinimidyl-4-azidotetrafluorobenzoate (2.00 g, 6.02 mmol) in 25 mL acetonitrile was added dropwise over 20 min. The reaction was stirred at 0 °C for an additional 1 h and the white precipitate that had formed filtered using a Buchner funnel. To the filtrate was added 100 mL chloroform and washed with water (3 × 50 mL) and dried over magnesium sulfate. The solvent was removed in vacuo and the solid was vacuum-dried to yield **1** (1.25 g, 75%) as a yellow solid. ¹H NMR (300 MHz, CDCl₃): δ 6.64 (br, 1H), 3.45 (m, 2H), 2.92 (m, 2H). ¹³C NMR (75 MHz, CDCl₃): δ 168.61, 160.25, 25.63.

Peptide Bond Formation for Scheme 2. A solution of EDC (2 mM) and NHS (5 mM) in activation buffer was freshly prepared prior to each reaction. Approximately 200 μL of the EDC/NHS solution was drop coated over the carboxyl-terminated polymer substrates. The reaction reached completion after 15 min and the excess EDC/NHS was removed by rinsing with copious amounts of coupling buffer.

TFPA Azide Molecule Deposition. TFPA azide molecule was deposited by placing the plasma modified (PS H) and EDC/NHS activated (PS R) polystyrene samples in 4 mM TFPA solution for two hours at room temperature. It should be noted that the time needed for sufficient deposition and the optimal TFPA concentration were empirically optimized. Dip coating for more than two hours allows for increased physisorption and was not beneficial for graphene transfer. Angle-resolved XPS analysis of deposition of higher molarity TFPA solutions suggested multilayers, rather than monolayer formation. The surfaces were extensively rinsed and sonicated for 10 min in methanol and finally dried with nitrogen. Prior to print, the azide-coated polymers are stored in a nitrogen glovebox with no exposure to direct sun light. The prepared PS H and PS R surfaces before print are stable and can be used whenever needed.

Direct Transfer Print. The transfer print of PS H, PS R, and PS ref samples was performed using a NX 2000 Nano Imprint machine at a pressure of 500 psi for 30 min at a temperature of 150 °C.

Raman Spectroscopy and Micro-Raman Maps. Raman spectra were acquired using a Renishaw InVia Raman microscope with a constant power of 20 mW of power and exposure time of 20 s. A Horiba, LabRAM ARAMIS Confocal Raman microscope equipped with 532 nm laser was used for the micro-Raman maps. The microscope was calibrated to the 520.7 cm⁻¹ peak of a silicon (111) wafer to within ±2 cm⁻¹ prior to each measurement. All measurements used an exposure time of 10 s and were averaged over two exposures. The spot size of the laser when focused on the sample surface is approximately 1 μm. The DuoScan feature of the ARAMIS microscope was used to raster the laser spot over a 2 μm square. A general bandwidth of 100 cm⁻¹ for polystyrene centered at the peak maximum with the baseline removed was used for integration. Peak selection and integration were performed with LabSpec 5 version 5.55.10 software provided by Horiba Scientific.

Hall Effect Measurements. Hall effect mobility and carrier density measurements were carried out at 300 K using copper pressure clips in van der Pauw configuration. The clips were used as probe contacts over areas of 0.5 × 0.5 mm². The currents used for the measurements were 1 and 50 μA, while the magnetic field was approximately 2 kG.

■ ASSOCIATED CONTENT

Supporting Information

XPS spectra of reference and CO₂ plasma-treated polystyrene, photographs, and optical microscope images of graphene films. This material is available free of charge via the Internet at <http://pubs.acs.org>.

■ AUTHOR INFORMATION

Corresponding Author

*Phone: 202-767-0351. Fax: 202-767-3553. E-mail: evgeniya.lock@nrl.navy.mil.

■ ACKNOWLEDGMENTS

We thank W.E. Amatucci for the images of graphene on Si wafers and D. K. Gaskill and V. D. Wheeler for the use of the Hall Probe measurements system. The work was supported by the Naval Research Laboratory Base Program. M.B. and S.C.H. are grateful for the NRL/NRC Postgraduate research fellowship. J.T. and M.S.F. acknowledge support from the Laboratory for Physical Sciences and use of the UMD-MRSEC Shared Equipment Facilities under Grant DMR 05-20471. M.B. and S.C.H are NRL/NRC Postdoctoral Research Associates.

■ REFERENCES

- (1) Forrest, S. R. The path to ubiquitous and low-cost organic electronic appliances on plastic. *Nature* **2004**, *428*, 911–918.
- (2) Sheraw, C. D.; Zhou, L.; Huang, J. R.; Gundlach, D. J.; Jackson, T. N.; Kane, M. G.; Hill, I. G.; Hammond, M. S.; Campi, J.; Greening, B. K.; Francl, J.; West, J. Organic thin-film transistor-driven polymer-dispersed liquid crystal displays on flexible polymeric substrates. *Appl. Phys. Lett.* **2002**, *80* (6), 1088–1090.
- (3) Dimitrakopoulos, C. D.; Malenfant, P. R. L. Organic thin film transistors for large area electronics. *Adv. Mater.* **2002**, *14* (2), 99–117.
- (4) Hines, D. R.; Mezheny, S.; Breban, M.; Williams, E. D.; Ballarotto, V. W.; Esen, G.; Southard, A.; Fuhrer, M. S. Nanotransfer printing of organic and carbon nanotube thin-film transistors on plastic substrates. *Appl. Phys. Lett.* **2005**, *86*, 163101.
- (5) Hoppe, H.; Sariciftci, N. S. Organic solar cells: an overview. *J. Mater. Res.* **2004**, *19* (7), 1924–1945.
- (6) Warta, W.; Stehle, R.; Karl, N. Ultrapure, high mobility organic photoconductors. *Appl. Phys. A* **1985**, *36*, 163–170.
- (7) Burrows, P. E.; Forrest, S. R. Electroluminescence from trap-limited current transport in vacuum deposited organic light emitting devices. *Appl. Phys. Lett.* **1994**, *64*, 2285–2287.
- (8) Schwierz, F. Graphene transistors. *Nat. Nanotechnol.* **2010**, *5*, 487–496.
- (9) Bonaccorso, F.; Sun, Z.; Hasan, T.; Ferrari, A. C. Graphene photonics and optoelectronics. *Nat. Photonics* **2010**, *4*, 611–622.
- (10) Wassei, J. K.; Kaner, R. B. Graphene, a promising transparent conductor. *Mater. Today* **2010**, *13* (3), S2–S9.
- (11) Arco, L. G. D.; Zhang, Y.; Schlenker, C. W.; Ryu, K.; Thompson, M. E.; Zhou, C. Continuous, Highly Flexible, and Transparent Graphene Films by Chemical Vapor Deposition for Organic Photovoltaics. *ACS Nano* **2010**, *4* (5), 2865–2873.
- (12) Matyba, P.; Yamaguchi, H.; Eda, G.; Chhowalla, M.; Edman, L.; Robinson, N. D. Graphene and Mobile Ions: The Key to All-Plastic, Solution-Processed Light-Emitting Devices. *ACS Nano* **2010**, *4* (2), 637–642.
- (13) Li, X.; Cai, W.; An, J.; Kim, S.; Nah, J.; Yang, D.; Piner, R.; Velamakanni, A.; Jung, I.; Tutuc, E.; Banerjee, S. K.; Colombo, L.; Ruoff, R. S. Large-area synthesis of high-quality and uniform graphene films on copper foils. *Science* **2009**, *324*, 1312–1314.
- (14) Bae, S.; Kim, H.; Lee, Y.; Xu, X.; Park, J.-S.; Zheng, Y.; Balakrishnan, J.; Lei, T.; Kim, H. R.; Song, Y. I.; Kim, Y.-J.; Kim, K. S.; Ozyilmaz, B.; Ahn, J.-H.; Hong, B. H.; Iijima, S. Roll-to-roll production

of 30-in. graphene films for transparent electrodes. *Nat. Nanotechnol.* **2010**, *5*, 574–578.

(15) Verma, V. P.; Das, S.; Lahiri, I.; Choi, W. Large-area graphene on polymer film for flexible and transparent anode in field emission device. *Appl. Phys. Lett.* **2010**, *96*, 203108.

(16) Regan, W.; Alem, N.; Aleman, B.; Geng, B.; Girit, C.; Maserati, L.; Wang, F.; Crommie, M.; Zettl, A. A direct transfer of large-area graphene. *Appl. Phys. Lett.* **2010**, *96*, 113102.

(17) Kim, K. S.; Zhao, Y.; Jang, H.; Lee, S. Y.; Kim, J. M.; Kim, K. S.; Ahn, J.-H.; Kim, P.; Choi, J.-Y.; Hong, B. H. Large-scale pattern growth of graphene films for stretchable transparent electrodes. *Nature* **2009**, *457*, 706–710.

(18) Caldwell, J. D.; Anderson, T. J.; Culbertson, J. C.; Jernigan, G. G.; Hobart, K. D.; Kub, F. J.; Tadjier, M. J.; Tedesco, J. L.; Hite, J. K.; Mastro, M. A.; Myers-Ward, R. L.; Eddy, C. R.; Campbell, P. M.; Gaskill, D. K. Technique for the Dry Transfer of Epitaxial Graphene onto Arbitrary Substrates. *ACS Nano* **2010**, *4* (2), 1108–1114.

(19) Lee, Y.; Bae, S.; Jang, H.; Jang, S.; Zhu, S.; Sim, S. H.; Song, Y. I.; Hong, B. H.; Ahn, J.-H. Wafer-Scale Synthesis and Transfer of Graphene Films. *Nano Lett.* **2010**, *10*, 490–493.

(20) Song, L.; Ci, L.; Gao, W.; Ajayan, P. M. Transfer Printing of Graphene Using Gold Film. *ACS Nano* **2009**, *3* (6), 1353–1356.

(21) Lock, E. H.; Petrovykh, D. Y.; Mack, P.; Carney, T.; White, R. G.; Walton, S. G.; Fernsler, R. F. Surface Composition, Chemistry and Structure of Polystyrene Modified by Electron-Beam-Generated Plasma. *Langmuir* **2010**, *26* (11), 8857–8868.

(22) Liu, L. H.; Yan, M. Simple Method for Covalent Immobilization of Graphene. *Nano Lett.* **2009**, *9*, 3375–3378.

(23) Liu, L.; Engelhard, M. H.; Yan, M. Surface and Interface Control on Photochemically Initiated Immobilization. *J. Am. Chem. Soc.* **2006**, *128*, 14067–14072.

(24) Graf, D.; Molitor, F.; Ensslin, K.; Stampfer, C.; Jungen, A.; Hierold, C.; Wirtz, L. Spatially Resolved Raman Spectroscopy of Single- and Few-Layer Graphene. *Nano Lett.* **2007**, *7* (2), 238–242.

(25) Ferrari, A. C.; Meyer, J. C.; Scardaci, V.; Casiraghi, C.; Lazzeri, M.; Mauri, F.; Piscanec, S.; Jiang, D.; Novoselov, K. S.; Roth, S.; Geim, A. K. Raman spectrum of graphene and graphene layers. *Phys. Rev. Lett.* **2006**, *97*, 187401–1–187401–4.

(26) Suk, J. W.; Kitt, A.; Magnuson, C. W.; Hao, Y.; Ahmed, S.; An, J.; Swan, A. K.; Goldberg, B. B.; Ruoff, R. S. Transfer of CVD-Grown Monolayer Graphene onto Arbitrary Substrates. *ACS Nano* **2011**, *5* (9), 6916–6924.